ISBN: 978-3-95450-184-7 doi:10.18429/JACoW-IPAC2018-WEPAL028

STUDY OF THE INFLUENCE OF THE CSR IMPEDANCE ON THE SYNCHRONOUS PHASE SHIFT AT KARA

P. Schönfeldt*, B. Kehrer†, E. Blomley, M. Brosi, E. Bründermann, J. Gethmann, A. Papash, J. L. Steinmann, and A.-S. Müller
Karlsruhe Institute of Technology, Karlsruhe, Germany

Abstract

Measurements of the bunch current dependent synchronous phase shift are a standard method to characterize the impedance of a storage ring. To study this shift, different experimental approaches can be used. In this contribution, we first derive the phase shift caused by the impedance describing the emission of coherent synchrotron radiation (CSR) based on numerical simulations of the longitudinal phase space. The predicted shift is compared to measurement results, obtained by time-correlated single photon counting.

INTRODUCTION

A crucial parameter to understand and eventually prevent instabilities in an accelerator is the impedance. We are particularly interested in the micro-bunching instability which is caused by the CSR impedance. As a direct measurement of the impedance is not feasable, it can only be investigated by studies of impedance-related effects. For the resistive (real) part of the impedance, one of these effects is the current dependent shift of the synchronous phase. For a single particle, the synchronous phase is defined by the energy balance between accelerating voltage V_{RF} and synchrotron radiation losses U_0. In a classical view that neglects the quantum nature of radiation, an electron at the synchronous phase

$$\Psi_0 := \arcsin\left(\frac{U_0}{eV_{\mathrm{RF}}}\right) \tag{1}$$

will stay at this fixed phase relation with respect to the accelerating voltage. For electron bunches with charge $|Q| > |e|$ however, there are additional losses U_{C} due to collective effects. An electron's total energy budget per revolution can then be expressed as

$$\Delta E + eV_{\mathrm{RF}}\left[\sin(\Psi) - \sin(\Psi_0)\right] = U_0 + U_{\mathrm{C}}. \tag{2}$$

U_{C} is a function not only of the bunch charge $Q = eN$ and the impedance Z, but also of the position $\tau = \Psi/(2\pi f_{\mathrm{RF}})$ of the particle with respect to the synchronous phase in the zero-current limit and of the Fourier transform of the bunch profile $\tilde{\rho}(\omega) = \int_{-\infty}^{\infty} \rho(\tau) e^{-i\omega\tau} \mathrm{d}\tau$ [1]

$$U_{\mathrm{C}}(\tau) = \frac{e^2 N}{2\pi} \int_{-\infty}^{\infty} Z(\omega)\, \tilde{\rho}\,(\omega)\, e^{i\omega\tau} \mathrm{d}\omega. \tag{3}$$

Averaging over all particles $\int_{-\infty}^{\infty} \rho \, \mathrm{d}\tau$ yields

$$\langle U_{\mathrm{C}} \rangle = \frac{e^2 N}{2\pi} \int_{-\infty}^{\infty} \Re[Z\,(\omega)]\, |\tilde{\rho}\,(\omega)\,|^2 \mathrm{d}\omega = k e^2 N, \tag{4}$$

There are two common approximations: where k is the loss factor. Typically, this quantity is taken for U_{C} in Eq. (2), resulting in an average phase $\langle\phi\rangle = \langle\Psi\rangle - \Psi_0$, which is equivalent to the center of mass position of the bunch. For small phase variations $\phi \ll 1$, it is $\sin(\Psi) - \sin(\Psi_0) \approx \phi \cos\Psi_0$. This is done, e.g. in [2]. Also, when $\partial\rho/\partial Q = 0$, $k(Q)$ is constant and $\phi \propto Q$, as in [3]. Notice that dependent on the shape of Z, $k(Q)$ can also be constant with changing $\rho(Q)$. Alternatively to using Eq. (4), one can directly utilize Eq. (3). In this view, the synchronous phase ϕ_0 is defined by an individual particle with $\Delta E = 0$. As it is part of the ensemble, $U_{\mathrm{C}} \neq 0$ and $\phi_0 \neq \Psi_0$. For a strong potential well distortion, there can also be a significant difference between ϕ_0 and $\langle\phi\rangle$. It is noteworthy that the incoherent (single-particle) synchrotron motion is around the first, while coherent (complete bunch) synchrotron motion is around the latter.

SIMULATIONS

We know [4] that for short-bunch operation at the KArlsruhe Research Accelerator (KARA) at KIT, the beam dynamics can be modeled reasonably well using Z_{PP}, the CSR impedance shielded by parallel plates [5]. An example configuration, that is used for this contribution, can be seen in Tab. 1. To find the contribution of this impedance to the phase shift, we use the simulation code Inovesa [6]. Scripts to reproduce the simulation results can be found at [7]. Carrying out simulation runs over a wide current

Table 1: KARA parameters and settings. Starting from V_{RF}, all quantities can be flexibly adjusted for the experiment.

Quantity	Symbol	Value	Unit
Revolution frequency	f_{rev}	2.716	MHz
Harmonic number	h	184	
Bending radius	R	5.559	m
Full beam pipe height	g	32	mm
Accelerating Voltage	V_{RF}	1.5	MV
Beam energy	E_0	1.285	GeV
Energy spread	σ_E	6040	keV
Damping time	τ_{d}	10.4	ms
Synchrotron frequency	$f_{\mathrm{s},0}$	11460	Hz

* patrik.schoenfeldt@kit.edu
† benjamin.kehrer@kit.edu

ISBN: 978-3-95450-184-7 doi:10.18429/JACoW-IPAC2018-WEPAL028

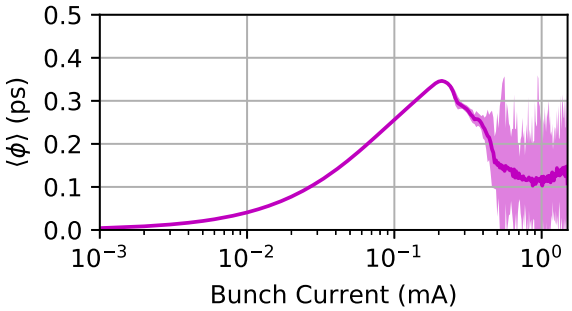

Figure 1: Simulated current-dependent bunch position. The standard deviation of the fluctuations in positions in bursting CSR is displayed as a band around the average value. The micro-bunching instability threshold is at $I_b \approx 0.18$ mA.

range yields the current-dependency of the average phase displayed in Fig. 1. The qualitative current-dependency of the synchronous phase is as follows: For stable conditions, the phase is not fluctuating but increases monotonically with current. As $\langle\phi\rangle \propto U_C$, this is also true for the average energy loss. In more detail, the form factor can be considered constant near $I_b = 0$, so here $U_C \propto I_b^2$. Bunch lengthening, however, counteracts the quadratic behavior. This can also be seen, e.g. in the phase shift measurements [2]. The general trend changes at the micro-bunching instability threshold. For the displayed data, it is reached at $I_b \approx 0.18$ mA. At this current, the bunch leans forward the most. Above, substructures form on the phase space and the micro-bunching instability leads to fluctuations in emissions and phase. In total, the average emission per particle decreases (this has been observed, e.g., at MLS [8]).

The case simulated here only takes into account the CSR impedance. While this impedance is assumed to dominate the high frequency range, there are additional contributions to the overall impedance budget of a storage ring like geometric impedances due to apertures and cavities as well as the resistive wall impedance due to the finite conductivity of the beam pipe. Independent of their nature (broad or narrow-band) these contributions are assumed to be dominant in the low-frequency range below 50 GHz, where the CSR is shielded. As the form factor is 1 close to $f = 0$ Hz, these contributions to the overall impedance might still dominate the coherent losses U_C. In that case, the curve shown in Fig. 1, is just one small contribution so that no peak will be observed in the phase shift.

EXPERIMENTAL METHODS

First of all, experimental studies of the phase shift require a precise timing reference. Ideally, the RF signal could be taken directly. However, for longer measurement times, e.g. temperature changes in the clock distribution can lead to significant timing drifts – we observed up to 10 ps. A common way to provide a more stable timing reference is the usage of additional bunches. Often, two bunches are observed for a long time: One bunch starts with high charge which decreases faster as the one of a low-charge reference bunch. When $k(Q) = const.$, it is then possible to determine the phase shift based on the differences of the two bunches in both, charge and phase. If the reference bunch is small enough, it might also have almost constant charge and thus assumed to stay at the same phase. For Z_{PP}, we see the problem that the phase of a low-current bunch might actually shift stronger then the one of the high-current bunch. A solution is a filling pattern persisting of multiple bunches spanning a wide range of charges – allowing to perform the measurement in a short period of time [$Q(t) \approx const.$]. To exclude influence of beam loading and other effects on the phase, the pattern has to be carefully designed. An example can be found in [2].

For the actual arrival time measurements, we utilize a setup based on time-correlated single photon counting which is located at the visible light diagnostics port [9]. This setup is used to determine the filling pattern of the storage ring [10]. To identify the arrival time, usually Gaussian curves are fitted to individual peaks in the histogram. If single photon avalanche diodes (SPAD) are used as detectors, the shape of these peaks deviates from a normal distribution due to detector effects [11]. Even if the *diffusion tail* can be minimized using bandpass filters, it cannot be suppressed completely. Therefore, we do not fit purely Gaussian curves but exponentially modified Gaussians [12]. Their probability density function can be written as

$$f_{\mathrm{EMG}} = \frac{\exp\left[\frac{1}{2}\left(\frac{\tilde{\sigma}}{\tilde{\tau}}\right)^2 - \frac{x-\tilde{\mu}}{\tilde{\tau}}\right]}{2\tilde{\tau}} \times \mathrm{erfc}\left(\frac{1}{\sqrt{2}}\left(\frac{\tilde{\sigma}}{\tilde{\tau}} - \frac{x-\tilde{\mu}}{\tilde{\sigma}}\right)\right).$$

It is defined by the position $\tilde{\mu}$ and the size $\tilde{\sigma}$ of the underlying Gaussian distribution as well as the time constant $\tilde{\tau}$ of the exponential decay; erfc is the complementary error function [13, Eq. 6.2.9].

The bunch arrival time can be determined from the first statistical moment which is given by $\tilde{\tau} + \tilde{\mu}$. Compared to a purely Gaussian fit, this function leads to better results as it is

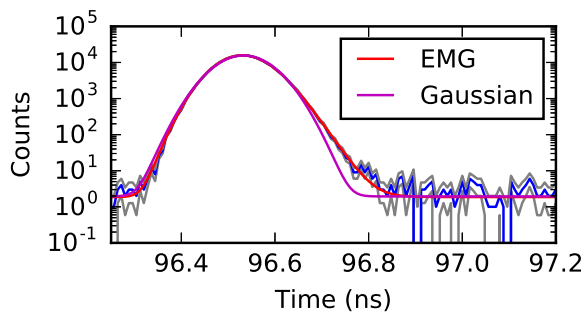

Figure 2: Raw data histogram (blue) and fits to the peak region using an exponentially modified Gaussian (EMG, red) and a Gaussian (purple). The grey lines show the $\pm 1\sigma$ band around the measurement data, calculated according to Poisson's statistics ($\sigma_i = \sqrt{n_i}$).

ISBN: 978-3-95450-184-7 doi:10.18429/JACoW-IPAC2018-WEPAL028

shown in Fig. 2. Already a comparison by eye shows that the exponentially modified Gaussian reproduces the shape of the peaks better. This is quantified by the value for the reduced chi-squared, which is 4.92 for the purely Gaussian while it is 1.01 for the exponentially modified Gaussian, respectively.

It is noteworthy that the shape of the bunch peaks is defined by the detector response. In case of the SPAD used here (id100-20 ULN [14]), the FWHM of the detector point-spread function is in the order of 40 ps, which is approximately one order of magnitude above the FWHM bunch length. In addition, the acquisition time is very long compared to a synchrotron period and thus the synchrotron motion is averaged out and the peak position only allows to identify the center of the oscillation – which corresponds to $\langle\phi\rangle$. To find ϕ_0, the bunch shape would have to be detected on a single-turn basis – for example using a streak camera with two time axes.

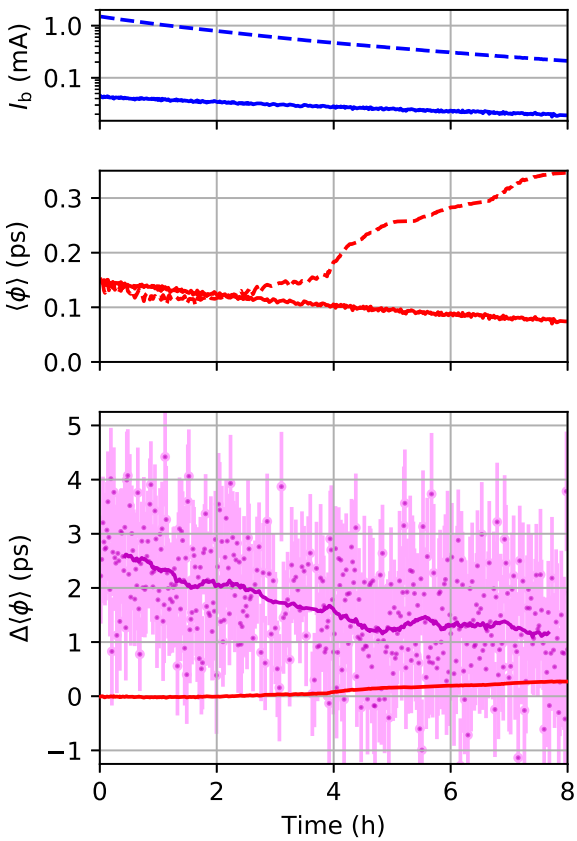

Figure 3: Upper: Currents (blue) of two example bunches and phase (red). Solid lines mark the low-charge bunch, the dashed ones the high-charge one. Lower: Individual measurements of phase difference (light magenta). To guide the eye, a moving average (magenta line) has been added. The red line gives the contribution by the phase shift computed based on the CSR impedance model (see upper plot and Fig. 1).

RESULTS

Using a custom filling pattern, we would have been restricted by our harmonic number of 184. Thus, we chose to stick to the approach observing the evolution of only two different bunches. However, having in mind the possibility of a significant drift of the *reference* bunch, we consider the two individual bunch currents. They start at 1.5 mA and 44 µA and go down to 202 µA and 19 µA, respectively. This method does not aim to find $k(Q)$ but allows to quantify to which extent the CSR impedance used for the simulation contributes to the total losses. Results of both, measurement and simulation are compared in Fig. 3. As expected, the phase of the smaller bunch shows a significant shift due to the CSR impedance. In the measurement, the effect is less important: The contribution of Z_{PP} to the total impedance budget seems to be small for high currents. However, it becomes significant for lower currents. For lower bunch currents, the overall losses will probably be dominated by the emission of CSR. That the influence is largest here is expected, as the bunches are shortest for these conditions.

SUMMARY

Aiming to find the influence of the CSR impedance to the total losses during the short-bunch operation at KARA, we compared different methods to define and to measure the synchronous phase. As we expect a significant phase shift also for small absolute current changes of a low-charge bunch, we took into account both individual bunch currents and compared measurement and simulation. Our results indicate, that for low bunch currents, and thus shorter bunches, the overall losses can be dominated by the emission of CSR. For higher currents, however, additional sources seem to dominate the total impedance.

ACKNOWLEDGEMENTS

Edmund Blomley and Julian Gethmann acknowledge the support by the DFG-funded Doctoral School "Karlsruhe School of Elementary and Astroparticle Physics: Science and Technology (KSETA)". Miriam Brosi, Patrik Schönfeldt and Johannes Steinmann acknowledge the support by the "Helmholtz International Research School for Teratronics (HIRST)".

This work has been supported by the German Federal Ministry of Education and Research (Grant No. 05K16VKA) and the Helmholtz Association (Contract No. VH-NG-320).

REFERENCES

[1] K. Y. Ng, "Physics of Intensity Dependent Beam Instabilities", *W*orld Scientific Publishing, 2006.

[2] G. Rehm, C. Bloomer, and C. Thomas, "Loss Factor Measurement Using Time Correlated Single Photon Counting of Synchrotron Radiation", in *P*roc. 10th European Workshop on Beam Diagnostics and Instrumentation for Particle Accelerators, Hamburg, Germany, May 2011, pp. 110–112.

[3] B. Podobedov and R. Siemann. "New apparatus for precise synchronous phase shift measurements in storage rings", in

ISBN: 978-3-95450-184-7 doi:10.18429/JACoW-IPAC2018-WEPAL028

Phys. Rev. ST Accel. Beams, Nov. 1998, vol. 1, p. 072801. doi:10.1103/PhysRevSTAB.1.072801

[4] M. Brosi et al. "Fast mapping of terahertz bursting thresholds and characteristics at synchrotron light sources", in *Phys. Rev. Accel. Beams*, Nov. 2016, vol. 19, p. 110701. doi:10.1103/PhysRevAccelBeams.19.110701

[5] J. Murphy, S. Krinsky, and R. Gluckstern, "Longitudinal wakefield for an electron moving on a circular orbit", in *Part. Accel.*, vol. 57, pp. 9-64, 1997.

[6] P. Schönfeldt, M. Brosi, M. Schwarz, J. L. Steinmann, and A.-S. Müller, "Parallelized Vlasov-Fokker-Planck solver for desktop personal computers", in *Phys. Rev. Accel. Beams*, vol. 20, p. 030704, 2017. doi:10.1103/PhysRevAccelBeams.20.030704

[7] "Inovesa examples", https://github.com/Inovesa/examples.

[8] J. Feikes et al., "Metrology Light Source: The first electron storage ring optimized for generating coherent THz radiation", in *Phys. Rev. ST Accel. Beams*, Mar. 2011, vol. 14, p. 030705. doi:10.1103/PhysRevSTAB.14.030705

[9] B. Kehrer et al., "Visible Light Diagnostics at the ANKA Storage Ring", in *Proc. IPAC'15*, Shanghai, China, May 2015, paper MOPHA037, pp. 866-868. doi:10.18429/JACoW-IPAC2015-MOPHA037

[10] B. Kehrer et al., "Filling Pattern Measurements Using Dead-Time Corrected Single Photon Counting", in *Proc. IPAC'18*, (WEPAL027), this conference.

[11] S. Cova et al., Review of Scientific Instruments 52.3 (1981): 408-412

[12] E. Grushka et al., Anal. Chem. 44, 11, pp. 1733-1738, 1972.

[13] W. H. Press et al., "Numerical recipes in C", Vol. 2., Cambridge university press, Cambridge, 1992.

[14] idQuantique website: http://idquantique.com